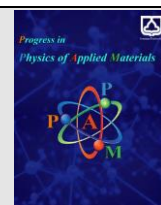




Semnan University

journal homepage: <https://ppam.semnan.ac.ir/>

# Pseudocapacitive performance of cobaltite and nickel cobaltite electrodes fabricated by layer-by-layer chemical deposition method

Mahdi Kazazi \*, Mohsen Mirzaie, Javad Rahimi Junaqani

Department of Materials Engineering, Faculty of Engineering, Malayer University, Malayer, Iran.

## ARTICLE INFO

### Article history:

Received: 6 August 2024

Revised: 13 August 2024

Accepted: 14 August 2024

### Keywords:

Nickel cobaltite

Chemical deposition

Binder-free electrode

Supercapacitors

## ABSTRACT

The development of efficient strategies for fabricating binder-free electrodes to electrochemical energy storage applications is of interest. Here, a novel approach of layer-by-layer chemical deposition was proposed for the preparation of binderless cobaltite ( $\text{Co}_3\text{O}_4$ ) and nickel cobaltite ( $\text{NiCo}_2\text{O}_4$ ) pseudocapacitive electrodes. The structure and morphology of the electrodes were obtained by X-ray diffraction (XRD) and field emission scanning electron microscopy (FESEM) examinations. The results demonstrated that the active materials were uniformly deposited on the surface of the nickel current collector. Also, a more porous structure was obtained in the case of nickel cobaltite electrode, which could improve the diffusion of ions to the active materials. Pseudocapacitive performance of the electrodes was obtained by cyclic voltammetry (CV), galvanostatic charge-discharge (GCD) and electrochemical impedance spectroscopy (EIS) measurements. The results demonstrated that the nickel cobaltite electrode exhibited superior charge storage performance including a high specific capacitance of  $1251 \text{ F g}^{-1}$  at  $1 \text{ A g}^{-1}$  and good rate capability (89.7% capacitance retention with a 10-fold increase in the current rate), which were higher than those for the cobaltite electrode.

## 1. Introduction

Recently, renewable energy storage devices have been of interest owing to the environmental pollution of fossil fuels. High-potential supercapacitors, for energy storage, are extremely important among the other energy storage power sources due to their exceptional storage characteristics and high power rates compared to conventional capacitors. High power density, long cycling stability, and acceptable energy storage capacity have filled the gap between batteries and traditional capacitors [1-5].

Supercapacitors are divided into three groups: oxidation-reduction supercapacitors (pseudocapacitors), electrolytic double-layer supercapacitors, and hybrid supercapacitors. The first group uses electroactive materials such as metal oxides and conductive polymers; the second group includes various allotropes of carbon, and the third group is a combination of the first and second groups [6-10]. Considering that the properties of the

supercapacitor are dependent on the type of electrode, identifying and choosing the right materials for the supercapacitors electrode requires special attention. Metal oxides like  $\text{RuO}_2$ ,  $\text{MnO}_2$ ,  $\text{NiO}$ , and many two-component transition metal oxides such as  $\text{NiCo}_2\text{O}_4$ ,  $\text{MnCo}_2\text{O}_4$ ,  $\text{CuCo}_2\text{O}_4$ , and  $\text{NiFe}_2\text{O}_4$  have been used as electrode materials for pseudocapacitors. Among various metal oxides, ruthenium oxide has attracted much attention due to its high specific capacitance. However, due to its high price, research is ongoing on other alternative metal oxides with lower price and abundance in nature [11-18].

Cobaltite is one of the most interesting active materials used in supercapacitors and its theoretical capacitance is higher than that for other metal oxides. By leaving out ruthenium oxide owing to its high cost and toxicity compared to two widely used metal oxides, its conductivity is higher than  $\text{MnO}_2$  and lower than  $\text{NiO}$ . The three known types of cobalt oxides include  $\text{Co}_3\text{O}_4$ ,  $\text{Co}_2\text{O}_3$ , and  $\text{CoO}$  [19-21]. Obtaining this oxide in pure form is difficult due to the

\* Corresponding author.

E-mail address: [mahdi.kazazi@gmail.com](mailto:mahdi.kazazi@gmail.com)

### Cite this article as:

Kazazi, M., Mirzaie, M. and Rahimi Junaqani, J., 2024. Pseudocapacitive performance of cobaltite and nickel cobaltite electrodes fabricated by layer-by-layer chemical deposition method. *Progress in Physics of Applied Materials*, 4(2), pp.145-151. DOI: [10.22075/PPAM.2024.34952.1111](https://doi.org/10.22075/PPAM.2024.34952.1111)

© 2024 The Author(s). Progress in Physics of Applied Materials published by Semnan University Press. This is an open access article under the CC-BY 4.0 license. (<https://creativecommons.org/licenses/by/4.0/>)

easy absorption of oxygen even at room temperature and its conversion to oxide with a higher level of contained oxygen. This oxide absorbs a suitable amount of oxygen and transforms into a higher oxide without changing the lattice parameter. Among various cobalt oxides,  $\text{Co}_3\text{O}_4$  has been noticed in supercapacitor and battery research due to its high surface area, modifiable surface area, and good oxidation and reduction properties [22-25].

It has been demonstrated that adding nickel element to cobaltite material to prepare  $\text{NiCo}_2\text{O}_4$  with a spinel structure can improve its energy storage characteristics [26-29]. It is well known that adding nickel to cobalt oxide increases its electrical conductivity, improves surface morphology and reduces its particle size, thereby improving its electrochemical performance and energy storage characteristics. This has caused nickel cobaltite to be used as an active material in supercapacitors and lithium batteries as a replacement for cobaltite [30-32]. Several methods such as solvothermal, hydrothermal, chemical precipitation, and sol-gel have been used for the synthesis of cobaltite-based electrode materials. However, the obtained electroactive material using these methods must be combined with a binder such as polyvinylidene fluoride (PVDF) to coat on the surface of current collector. Due to the fact that the binder used in the traditional preparation of the electrode is insulated, the internal resistance of the electrode increases, and as a result, it causes a significant decrease in the practical specific capacitance compared to the theoretical specific capacitance of the electrode. Therefore, the development of an efficient method for preparing energy storage electrodes without using binders can significantly increase the energy storage capacitance and the rate capability of the electrode.

In this study, the cobaltite and nickel cobaltite electrodes were fabricated by a simple layer-by-layer chemical deposition technique. The morphological, structural, and electrochemical properties of the as-fabricated electrodes were characterized in detail.

## 2. Experimental

### 2.1. Preparation of the cobaltite-based electrodes

Before depositing on the substrate, the graphite sheet current collector must be free of any contamination. Hence, the graphite sheet was cut in dimensions of  $1 \times 1 \text{ cm}^2$  and then rinsed in distilled water and alcohol, and finally dried.

To prepare a cobaltite electrode, cobalt hydroxide was first deposited on the surface of graphite substrate by a step-by-step chemical deposition method. This work was done by step-by-step and through successive immersion in three aqueous solutions as described below:

**Solution 1:** The first solution contains 1 ml of ammonia ( $\text{NH}_3$ ) dissolved in 24 ml of distilled water.

**Solution 2:** The second solution includes 0.2 M of hexahydrate cobalt nitrate salt (to create a pure cobalt oxide coating) and 2.5 g of polyethylene glycol (PEG) dissolved in 25 ml of distilled water.

**Solution 3:** The third solution contains 25 ml of pure distilled water. It should be noted that the temperature of the first and second solution was at ambient temperature and the third solution was at  $40^\circ\text{C}$ , which was obtained by trial and error and with numerous tests.

For the fabricating of the nickel cobaltite electrode, all steps are the same as preparing the cobaltite electrode but in the second solution, instead of 0.2 M of cobalt nitrate, 0.066 M of nickel nitrate and 0.0134 M of cobalt nitrate were used.

For coating, the graphite sheet was immersed in the first solution for 5 seconds, in the second solution for 15 seconds, and in the third solution for 15 seconds. Then it was completely dried by a laboratory dryer. This cycle is repeated for the required number of times to achieve the desired layer thickness. After finishing the steps, the desired substrate is washed with deionized water so that the loose particles are removed and the desired uniform coating remains. Then the resulting electrode was dried at a temperature below  $100^\circ\text{C}$  and again, the dried electrode was calcined at a temperature of  $300^\circ\text{C}$  for 2 hr to finally obtain an oxide coating of spinel cobaltite and nickel cobaltite.

### 2.2. Film characterization and electrochemical measurements

The structure and phase of the as-prepared electrode materials were obtained by X-ray diffraction (XRD, Unisantis XMD-300). The surface morphology of the electrodes was examined using a field-emission scanning electron microscope (FESEM, Mira 3-XMU).

The electrochemical characteristics of the cobaltite and nickel cobaltite pseudocapacitor electrodes were investigated by cyclic voltammetry (CV), galvanostatic charge/discharge (GCD), and impedance spectroscopy in a three-electrode cell containing 2 M KOH aqueous electrolyte. Also, the cell contained a standard Ag/AgCl reference electrode and a platinum sheet counter electrode. The CV examination was carried out between 0 to 0.8 V (vs. Ag/AgCl) at various scan rates of 5 to  $50 \text{ mV s}^{-1}$ . Furthermore, electrochemical impedance spectroscopy (EIS) measurements were performed in a frequency range of 100 KHz to 10 MHz with a potential amplitude of  $\pm 10 \text{ mV}$ .

## 3. Results and discussion

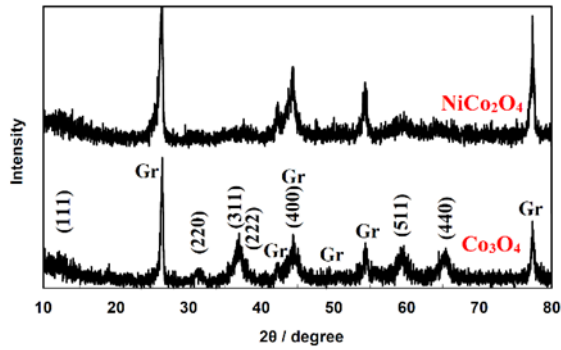
### 3.1. Electrode characterization

Fig. 1 shows the XRD pattern from the surface of cobaltite and nickel cobaltite electrodes. As can be seen, the XRD patterns of both electrodes are similar and both have peaks related to the graphite substrate. Also, the other peaks shown, which are related to the electrodeposited film, can be attributed to their spinel structure (JCPDS No: 42-1467) [33-35].

Furthermore, the crystalline size of the prepared active materials was calculated using Scherer's equation [36]:

$$d = (0.9 \times \lambda) / (w \times \cos \theta) \quad (1)$$

Where  $d$  is the average size of the crystals,  $\lambda$  is the Cu  $K\alpha$  wavelength (0.154 nm),  $\theta$  is the Bragg diffraction angle, and  $w$  is the peak width at half the peak intensity in radians. According to the calculations using the (220) crystal plane, the crystalline sizes of cobaltite and nickel cobaltite active materials were obtained as 17.2 and 20.4 nm, respectively.



**Fig. 1.** XRD patterns of the  $\text{Co}_3\text{O}_4$  and  $\text{NiCo}_2\text{O}_4$  electrodes.

To determine the structure, porosity, and size distribution of particles, a microscopic examination was performed using a scanning electron microscope. The FESEM images of the as-fabricated  $\text{Co}_3\text{O}_4$  and  $\text{NiCo}_2\text{O}_4$  electrodes were shown in Figure 2 (a,b) and Figure 3 (a,b), respectively. In the given images, we can see the presence of nanoparticles in the range of 1 micrometer to 500 nanometers on the graphite substrate. Images can be illustrated that cobalt oxide is made up of irregular and repeatable layers of different sizes. As can be seen, the cobalt oxide nanoparticles are scattered and uniformly distributed over the entire surface of the substrate. In contrast, the nickel cobaltite electrode presents a more porous structure. The porous structure of the nickel cobaltite electrode can improve the permeability of electrolyte ions within the electrode structure and leads to the improvement of the electrochemical usage of the active material and the increase of its rate capability. Furthermore, the nickel cobaltite electrode shows a structure with less agglomeration and the results show that the addition of nickel to the cobaltite material has improved the structural and morphological characteristics for energy storage application.

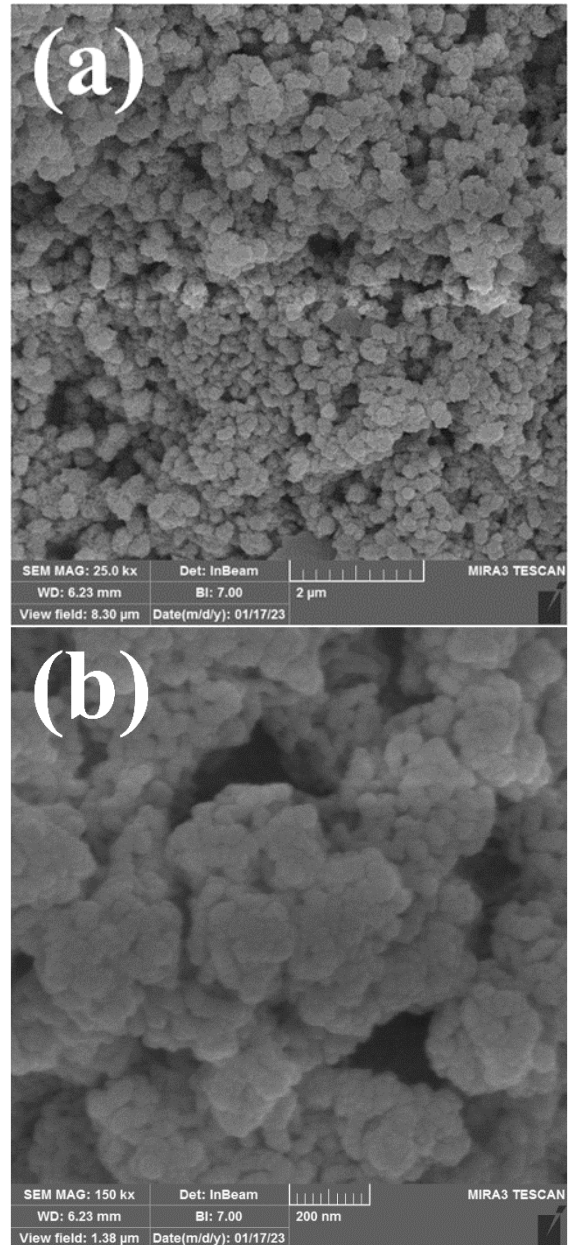


**Fig. 2.** FESEM images of the  $\text{Co}_3\text{O}_4$  electrode.

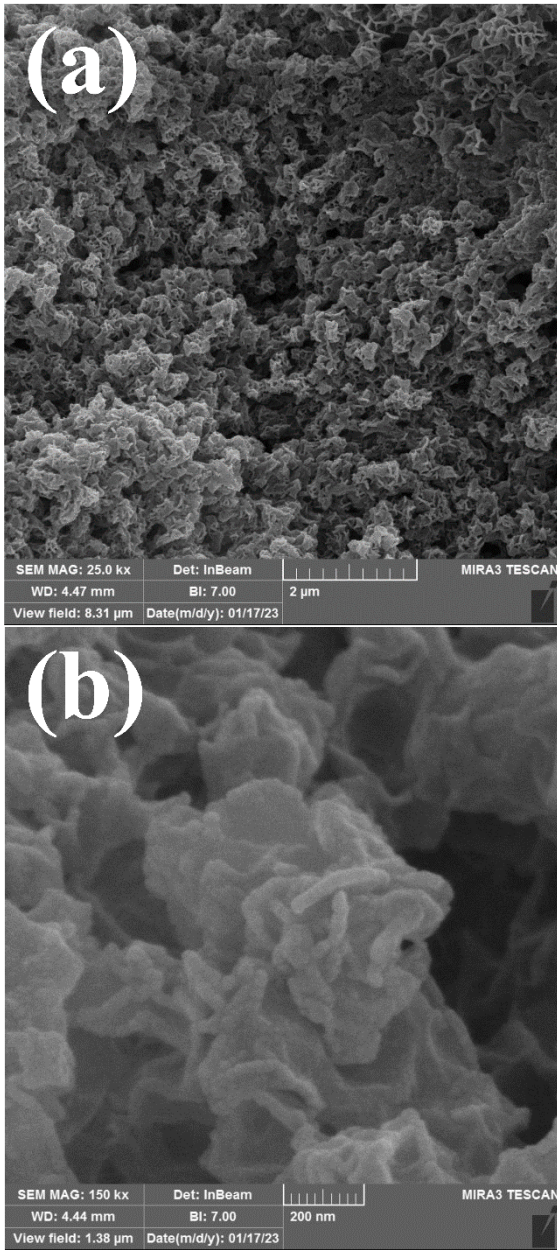
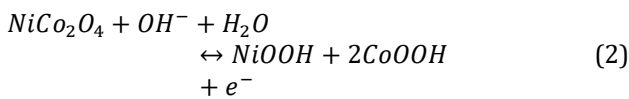


Fig. 3. FESEM images of the NiCo<sub>2</sub>O<sub>4</sub> electrode.

3.2. Electrochemical measurements

Fig. 4(a) depicts CV curves of both electrodes at a scanning rate of 20 mV s<sup>-1</sup>. It can be clearly seen that both coated electrodes demonstrate two reversible oxidation/reduction peaks, which represent their pseudocapacitive characteristics. The redox peaks in the CV curves are assigned to the reversible electrochemical reaction mechanism of nickel cobaltite in the alkaline electrolyte as follow [17]:



The greater the area under the voltammetry curve, the greater the specific capacity of the electrode. As can be seen, the nickel cobaltite electrode presents a larger area under the CV curve under similar scan rate, showing its higher specific capacitance related to the cobaltite electrode. For more investigation, CV curves of the cobaltite

and nickel cobaltite electrodes at various scanning rates of 5 to 50 mV s<sup>-1</sup> were shown in Figure 4(b) and (c), respectively. It can be seen that the potential difference between the anodic and cathodic peaks in the nickel cobaltite electrode is less than that in the cobaltite electrode, which indicates the better reversibility of the NiCo<sub>2</sub>O<sub>4</sub> electrode. The better reversibility of the NiCo<sub>2</sub>O<sub>4</sub> electrode can be attributed to the better kinetics of charge transfer and ion transfer within the electrode structure, which is obtained due to its porous structure with higher conductivity [37].

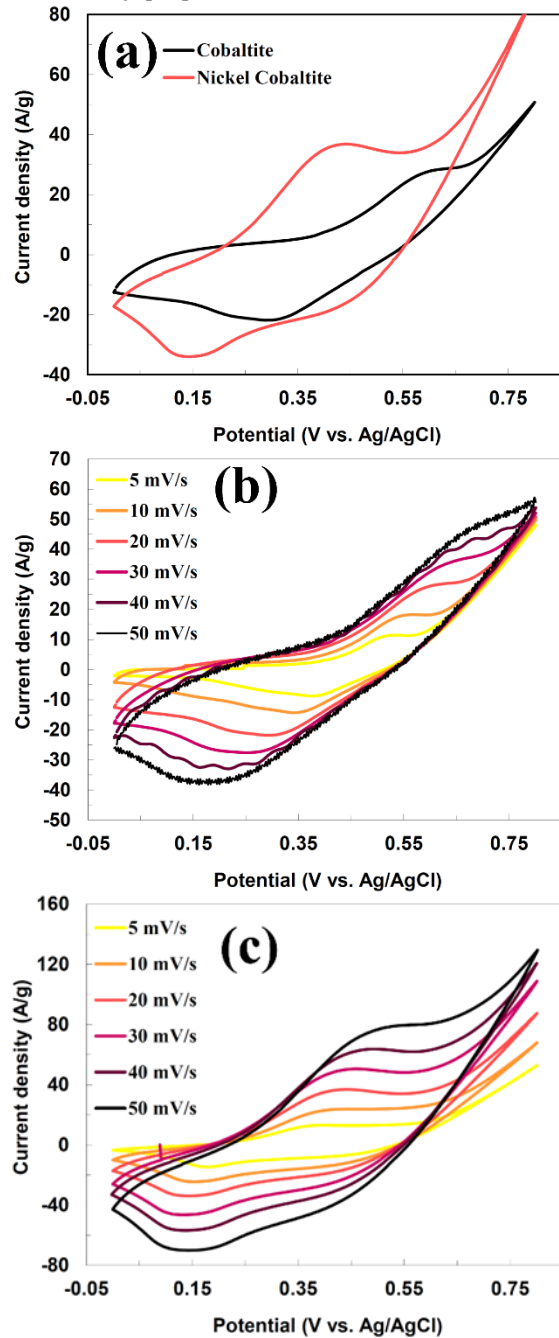


Fig. 4. (a) CV curves of the cobaltite and nickel cobaltite electrodes at a scan rate of 20 mV s<sup>-1</sup>; CV curves of the (b) cobaltite and (c) nickel cobaltite electrodes at different scan rates.

A GCD measurement was performed to further evaluate the capacitive performance of both electrodes. The GCD curves of the cobaltite and nickel cobaltite electrodes at various current rates from 1 to 10 A g<sup>-1</sup> are shown in Figure

5(a) and (b), respectively. As clearly seen, both electrodes have a stable voltage plateau during both the charge and discharge processes. It should be noted that the stable voltage plateaus observed in the GCD curves are in complete agreement with the oxidation and reduction peaks observed in the CV curves (Fig. 4(a)). The presence of these stable voltage plateaus in the GCD curves is characteristic of the pseudocapacitive behavior of the electrodes. Moreover, it is clearly seen that the nickel cobaltite electrode shows a lower IR drop in the discharge curves compared to the cobaltite electrode, which means a lower charge transfer resistance for the nickel cobaltite electrode.

The specific capacitances of the cobaltite and nickel cobaltite electrodes were calculated using the following equation and are shown in Figure 7c:

$$C_s = (i \times \Delta t) / (m \times \Delta V) \quad (3)$$

Where  $i$  is the discharge current (A),  $\Delta t$  is the discharge time (s),  $m$  is the mass of the electrode material, and  $\Delta V$  is the potential window (V). As shown in Figure 5(c), the nickel cobaltite electrode has much higher specific capacitances (1251, 1246, 1243, 1191, and 1122 F g<sup>-1</sup>, respectively) compared to the cobaltite electrode (791, 776, 762, 741, and 691 F g<sup>-1</sup>) respectively at current densities of 1, 2, 3, 5, and 10 A g<sup>-1</sup>. Furthermore, the capacity retention with a 10-fold increase in current density in the nickel cobaltite electrode is 89.7%, which is higher than that for the pure electrode (87.3%). The improved specific capacitance and the better rate performance of the nickel cobaltite electrode can be attributed to the improvement of electrical conductivity and the increase in the diffusion rate of electrolyte ions within the electrode structure.

The EIS measurements were carried out for the Co<sub>3</sub>O<sub>4</sub> and NiCo<sub>2</sub>O<sub>4</sub> electrodes before any electrochemical measurements. The Nyquist spectra of the Co<sub>3</sub>O<sub>4</sub> and NiCo<sub>2</sub>O<sub>4</sub> electrodes are presented in Figure 6(a). In the low-frequency range, the electrochemical impedance diagram appears as a Warburg, which is caused by the diffusion of ions. The shorter and steeper the line is, the faster the penetration of ions will be and if the angle of the Warburg line is closer to 90 degrees, it means that the behavior of the supercapacitor is very close to the ideal behavior. As can be seen in the diagram, the NiCo<sub>2</sub>O<sub>4</sub> electrode has a shorter length and a near vertical slope, while the Co<sub>3</sub>O<sub>4</sub> electrode has a longer length and a more inclined slope, so it shows that the penetration rate of ions in the NiCo<sub>2</sub>O<sub>4</sub> electrode is higher than in the Co<sub>3</sub>O<sub>4</sub> electrode. Quantitatively, the diffusion coefficient of electrolyte ions (D<sub>OH<sup>-</sup></sub>) can be calculated using the Warburg line in the low frequency region using the following equation [38]:

$$D_{Na^+} = 0.5 \left( \frac{RT}{An^2F^2\sigma_w C} \right)^2 \quad (4)$$

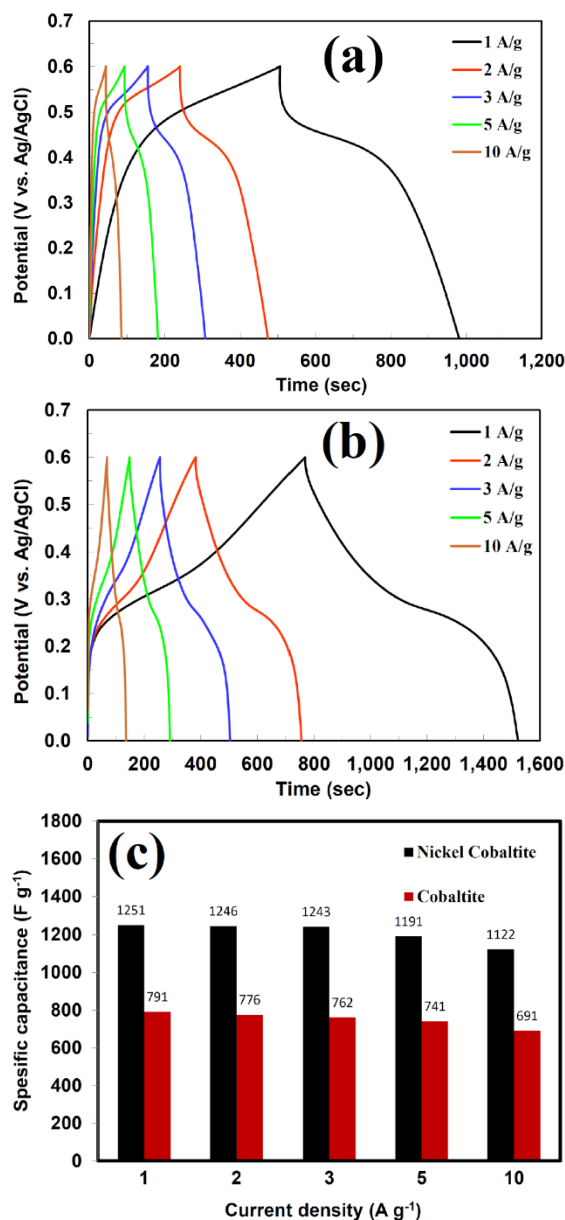


Fig. 5. Galvanostatic charge-discharge curves of the (a) cobaltite and (b) nickel cobaltite electrodes at various current rates; (c) Specific capacitance of the cobaltite and nickel cobaltite electrodes as a function of current rate.

Where  $R$  is the gas constant,  $T$  is the temperature,  $A$  is the surface area,  $n$  is the number of electrons during charge/discharge process,  $F$  is the Faraday's constant,  $C$  is the concentration of hydroxide ions in the electrolyte, and  $\sigma_w$  is the Warburg factor, which has the following relationship with real part of impedance ( $Z_{re}$ ) in the Warburg line region:

$$Z_{re} = R_D + R_L + \sigma_w \omega^{-1/2} \quad (5)$$

The linear plots between  $Z_{re}$  and the reciprocal square root of the angular frequencies ( $\omega^{-1/2}$ ) in the low frequency region for both the electrodes are shown in Figure 6(b). The diffusion coefficients of hydroxide ions are calculated to be  $9.2 \times 10^{-10}$  and  $3.15 \times 10^{-8}$  cm<sup>2</sup> s<sup>-1</sup> for the cobaltite and nickel cobaltite electrodes, respectively.

Furthermore, at high to medium frequencies, a square can be seen, which is associated with the charge transfer

resistance of the electrode. The larger the square diameter, the higher the internal resistance of the electrode, and conversely, the smaller the square diameter, the lower the internal resistance of the electrode. As can be seen in Figure 6, the nickel cobaltite electrode is seen in a smaller square, indicating its lower charge transfer resistance.

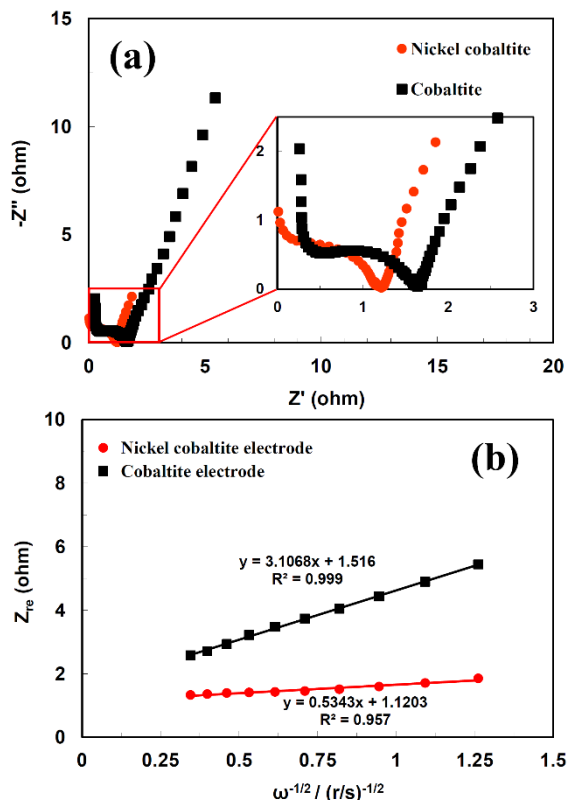


Fig. 6. (a) Nyquist spectra of the cobaltite and nickel cobaltite electrodes; (b) The relationship between  $Z_{re}$  and  $\omega^{-1/2}$  at low frequencies for the cobaltite and nickel cobaltite electrodes.

#### 4. Conclusion

In summary, the cobaltite and nickel cobaltite electrodes were fabricated using the layer-by-layer chemical precipitation method, and their pseudocapacitive performance was investigated in detail. Overall, the prepared nickel cobaltite electrode presented a better energy storage performance than the cobaltite electrode, which is due to its lower charge transfer resistance and higher ionic conductivity owing to its more porous structure, which facilitates the transfer of electrons and electrolyte ions to the active material, resulting to its better electrochemical utilization. The fabricated nickel cobaltite electrode exhibited a high specific capacitance of  $1251 \text{ F g}^{-1}$  at a current density of  $1 \text{ A g}^{-1}$  and excellent rate performance (capacitance retention of 89.7% with a 10-fold increase in current density), that they were all better than the cobaltite electrode.

#### Acknowledgements

The authors wish to express their gratitude to Malayer University for its support.

#### Conflicts of Interest

The author declares that there is no conflict of interest regarding the publication of this article.

#### References

- [1] Kazazi, M., 2019. High-performance electrode based on electrochemical polymerization of polypyrrole film on electrophoretically deposited CNTs conductive framework for supercapacitors. *Solid State Ionics*, 336, pp. 80–86.
- [2] Conway, B.E., 1999. *Electrochemical Supercapacitors. Scientific Fundamentals and Technological Applications*, Kluwer Academic/Plenum Press, New York.
- [3] Simon, P. and Gogotsi, Y., 2008. Material for electrochemical capacitors. *Nature. Materials*, 7, pp. 845–854.
- [4] Zhu, Y.W., Murali, S., Stoller, M.D., Ganesh, K.J., Cai, W.W., Ferreira, P.J., Pirkle, A., Wallace, R.M., Cychosz, K.A., Thommes, M., Su, D., Stach, E.A. and Ruoff, R.S., 2011. Carbon-based supercapacitors produced by activation of graphene. *Science*, 332, pp. 1537–1541.
- [5] Lee, J.W., Ahn, T., Soundararajan, D., Ko, J.M. and Kim, J.D., 2011. Non-aqueous approach to the preparation of reduced graphene oxide/ $\alpha$ -Ni(OH)<sub>2</sub> hybrid composites and their high capacitance behavior. *Chemical Communications*, 47, pp. 6305–6307.
- [6] Kazazi, M., 2019. High-performance electrode based on electrochemical polymerization of polypyrrole film on electrophoretically deposited CNTs conductive framework for supercapacitors. *Solid State Ionics*, 336, pp. 80–86.
- [7] Zhang, K., Zhang, L.L., Zhao, X.S. and Wu, J., 2010. Graphene/polyaniline nanofiber composites as supercapacitor electrodes. *Chemistry of Materials*, 22, pp. 1392–1401.
- [8] Frackowiak, E., Metenier, K., Bertagna, V. and Beguin, F., 2000. Supercapacitor electrodes from multi-walled carbon nanotubes. *Applied Physics Letters*, 77, pp. 2421–2423.
- [9] Kim, C. and Yang, K.S., 2003. Electrochemical properties of carbon nanofiber web as an electrode for supercapacitor prepared by electrospinning. *Applied Physics Letters*, 83, pp. 1216–1218.
- [10] Ghotbi, M.Y. and Azadfalsh, M., 2011. Design of a layered nanoreactor to produce nitrogen doped carbon nanosheets as highly efficient material for supercapacitors. *Chemical Communications*, 47, pp. 6305–6307.
- [11] Cottineau, T., Toupin, M., Delahaye, T., Brousse, T. and Belanger, D., 2006. Nanostructured transition metal oxides for aqueous hybrid electrochemical supercapacitors. *Applied Physics A*, 82, pp. 599–606.
- [12] Yuan, C., Wu, H.B., Xie, Y. and Lou, X.W.D., 2014. Mixed transition-metal oxides: design, synthesis, and energy-related applications. *Angewandte Chemie International Edition*, 53, pp. 1488–1504.
- [13] Mazinani, B., Kazazi, M., Mobarhan, G., and Shokouhimehr, M.R., 2019. The combustion synthesis of Ag-doped MnCo<sub>2</sub>O<sub>4</sub> nanoparticles for supercapacitor

- applications. *Journal of the Minerals, Metals and Materials*, 71, pp. 1499-1506.
- [14] Dubal, D.P., Lee, S.H., Kim, J.G., Kim, W.B. and Lokhande, C.D., 2012. Porous polypyrrole clusters prepared by electropolymerization for a high performance supercapacitor. *Journal of Materials Chemistry*, 22, pp. 3044-3052.
- [15] Wang, K., Zhang, X., Li, C., Zhang, H., Sun, X., Xu, N. and Ma, Y., 2014. Flexible solid-state supercapacitors based on a conducting polymer hydrogel with enhanced electrochemical performance. *Journal of Materials Chemistry*, 2, pp. 19726-19732.
- [16] Kazazi, M., 2017. Facile preparation of nanoflake-structured nickel oxide/carbon nanotube composite films by electrophoretic deposition as binder-free electrodes for high-performance pseudocapacitors. *Current Applied Physics*, 17, pp. 240-248.
- [17] Kazazi, M. and Karami, R., 2017. Hydrothermal synthesis and electrochemical characterization of mesoporous  $\text{Ni}_x\text{Co}_{3-x}\text{O}_4$  ( $0 \leq x \leq 1$ ) nanorods as electrode materials for high-performance electrochemical capacitors. *Solid State Ionics*, 308, pp. 8-15.
- [18] Kazazi, M., Sedighi, A.R. and Mokhtari, M.A., 2018. Pseudocapacitive performance of electrodeposited porous  $\text{Co}_3\text{O}_4$  film on electrophoretically modified graphite electrodes with carbon nanotubes. *Applied Surface Science*, 441, pp. 251-257.
- [19] Faraji, S. and Ani, F. N., 2014. Microwave-assisted synthesis of metal oxide/hydroxide composite electrodes for high power supercapacitors. *Journal of Power Sources*, 263, pp. 338-360.
- [20] Thota, S., Kumar, A. and Kumar, J., 2009. Optical, electrical and magnetic properties of  $\text{Co}_3\text{O}_4$  nanocrystallites obtained by thermal decomposition of sol-gel derived oxalates. *Materials Science and Engineering: B*, 164, pp. 30-37.
- [21] Guo, Q., Guo, X. and Tian, Q., 2010. Optionally ultra-fast synthesis of  $\text{CoO} / \text{Co}_3\text{O}_4$  particles using  $\text{CoCl}_2$  solution via a versatile spray roasting method. *Advanced Powder Technology*, 21, pp. 529-533.
- [22] Chen, J., Wu, X. and Selloni, A., 2011. Electronic structure and bonding properties of cobalt oxide in the spinel structure. *Physical Review B*, 245204, pp. 1-7.
- [23] Fang, H., Zhang, S., Liu, W., Du, Z., Wu, X. and Xing, Y., 2013. Hierarchical  $\text{Co}_3\text{O}_4$  multiwalled carbon nanotube nanocable films with superior cyclability and high lithium storage capacity. *Electrochimica Acta*, 108, pp. 651-659.
- [24] Deng, J., Kang, L., Bai, G., Li, Y., Li, P. and Liu, X., 2014. Solution combustion synthesis of cobalt oxides ( $\text{Co}_3\text{O}_4$  and  $\text{Co}_3\text{O}_4 / \text{CoO}$ ) nanoparticles as supercapacitor electrode materials. *Electrochimica Acta*, 132, pp. 127-135.
- [25] Wu, J.B., Lin, Y., Xia, X.H., Xu, J.Y. and Shi, Q.Y., 2011. Pseudocapacitive properties of electrodeposited porous nanowall  $\text{Co}_3\text{O}_4$  film. *Electrochimica Acta*, 56, pp. 7163-7170.
- [26] Zhu, Y., Ji, X., Wu, Z., Song, W., Hou, H., Wu, Z., He, X., Chen, Q. and Banks, C.E., 2014. Spinel  $\text{NiCo}_2\text{O}_4$  for use as a high-performance supercapacitor electrode material: understanding of its electrochemical properties. *Journal of Power Sources*, 267, pp. 888-900.
- [27] Wei, T.Y., Chen, C.H., Chien, H.C., Lu, S.Y. and Hu, C.C., 2010. A Cost-Effective Supercapacitor Material of Ultrahigh Specific Capacitances: Spinel Nickel Cobaltite Aerogels from an Epoxide-Driven Sol-Gel Process. *Advanced Materials*, 22, pp. 347-351.
- [28] Liu, Y., Wang, N., Yang, C. and Hu, W., 2016. Sol-gel synthesis of nanoporous  $\text{NiCo}_2\text{O}_4$  thin films on ITO glass as high-performance supercapacitor electrodes. *Ceramics International*, 42, pp. 11411-11416.
- [29] Chadwick, A.V., Savin, S.L.P., Fiddy, S., Alcantara, R., Lisbona, D.F., Lavela, P., Ortiz, G.F. and Tirado, J.L., 2007. Electrochemical Conversion Reaction of  $\text{NiFe}_2\text{O}_4$  Electrode as an Anode Material for Li-Ion Battery. *The Journal of Physical Chemistry C*, 111, pp. 4636-4642.
- [30] Wu, H.B., Pang, H. and Lou, X.W., 2013. Facile synthesis of mesoporous  $\text{Ni}_{0.3}\text{Co}_{2.7}\text{O}_4$  hierarchical structures for high-performance supercapacitors. *Energy & Environmental Science*, 6, pp. 3619-3626.
- [31] Rios, E., Nguyen-Cong, H., Marco, J.F., Gancedo, J.R., Chartier, P. and Gautier, J.L., 2000. Indirect oxidation of ethylene glycol by peroxide ions at  $\text{Ni}_{0.3}\text{Co}_{2.7}\text{O}_4$  spinel oxide thin film electrodes. *Electrochimica Acta*, 45, pp. 4431-4440.
- [32] Yuan, C., Li, J., Hou, L., Lin, J., Pang, G., Zhang, L., Lian, L. and Zhang, X., 2013. emplate-engaged synthesis of uniform mesoporous hollow  $\text{NiCo}_2\text{O}_4$  sub-microspheres towards high-performance electrochemical capacitors. *RSC Advances*, 3, pp. 18573-18578.
- [33] Huang, L., Zhang, W., Xiang, J. and Huang, Y., 2016. Porous  $\text{NiCo}_2\text{O}_4/\text{C}$  nanofibers replicated by cotton template as high-rate electrode materials for supercapacitors. *Journal of Materials*, 2, pp. 248-255.
- [34] Khalid, S., Cao, C., Ahmad, A., Wang, L., Tanveer, M., Aslam, I., Tahir, M., Idrees, F. and Zhu, Y., 2015. Microwave assisted synthesis of mesoporous  $\text{NiCo}_2\text{O}_4$  nanosheets as electrode material for advanced flexible supercapacitors. *RSC Advanced*, 5, pp. 33146- 33154.
- [35] Che, H., Liu, A., Mu, J., Bai, Y., Wu, C., Zhang, X., Zhang, Z. and Wang, G., 2017. Facile synthesis of flower-like  $\text{Ni}_x\text{Co}_{3-x}\text{O}_4$  ( $0 \leq x \leq 1.5$ ) microstructures as high-performance electrode materials for supercapacitors. *Electrochimical Acta*, 225, pp. 283-291.
- [36] Belkessam, C., Mechouet, M., Idiri, N., Kadri, A. and Djelali, N., 2019. Synthesis and characterization of  $\text{Ni}_{0.3}\text{Co}_{2.7}\text{O}_4$  oxide nanoparticles immobilized in Teflon cavity electrode for organic pollutants degradation. *Materials Research Express*, 6, pp. 105032.
- [37] Ding, R., Qi, L., Jia, M. and Wang, H., 2013. Facile and large-scale chemical synthesis of highly porous secondary submicron/micron-sized  $\text{NiCo}_2\text{O}_4$  materials for high-performance aqueous hybrid ACNiCo<sub>2</sub>O<sub>4</sub> electrochemical capacitors *Electrochimical Acta*, 107, pp. 494-502.
- [38] Kazazi, M. and Faryabi, M., 2020. Electrochemically anchored manganese hexacyanoferrate nanocubes on three-dimensional porous graphene scaffold: Towards a potential application in high-performance asymmetric supercapacitors. *Journal of Power Sources*, 449, pp. 227510.